



## Open Archive Toulouse Archive Ouverte (OATAO)

OATAO is an open access repository that collects the work of Toulouse researchers and makes it freely available over the web where possible.

This is an author-deposited version published in: <http://oatao.univ-toulouse.fr/>  
Eprints ID : 2342

**To link to this article :**

URL : <http://dx.doi.org/10.4028/www.scientific.net/MSF.595-598.213>

**To cite this version :** Vande Put, Aurélie and Oquab, Djar and Monceau, Daniel (2008) [\*Characterization of TBC systems with NiPtAl or NiCoCrAlYTaN bond coatings after thermal cycling at 1100°C: a comparative study of failure mechanisms.\*](#) Materials Science Forum, vol. 595 - 598 . pp. 213-221. ISSN 0255-5476

Any correspondence concerning this service should be sent to the repository administrator: [staff-oatao@inp-toulouse.fr](mailto:staff-oatao@inp-toulouse.fr)

# Characterization of TBC systems with NiPtAl or NiCoCrAlYTa bond coatings after thermal cycling at 1100°C: a comparative study of failure mechanisms

Aurélie VANDE PUT, Djar OQUAB, Daniel MONCEAU

CIRIMAT CNRS/UPS/INPT, ENSIACET, 118 Route de Narbonne, 31077 TOULOUSE  
cedex 4, France

Aurelie.VanDePut@ensiacet.fr, Djar.Oquab@ensiacet.fr; Daniel.Monceau@ensiacet.fr

**Keywords:** TBC, MCrAlY, NiPtAl, spallation, thermal cycling, thermogravimetry, failure mechanism, rumpling

**Abstract.** During service, TBC can suffer degradation by CMAS, FOD, erosion or spallation. Whereas the first three are due to foreign particles, the last one is related to thermal cycling. When subjected to high temperature exposures followed by rapid coolings under oxidizing conditions, a TBC system undergoes morphological changes and stress development. This will initiate cracks which propagate and finally lead to failure by spallation. Consequently, the aim of the present study is to understand better the mechanisms responsible for such spallation events. Two kinds of TBC systems with different bond coatings (NiCoCrAlYTa or Pt-modified nickel aluminide bond coatings) are thermally cycled. Subsequently, SEM investigations on TBC systems after spallation concentrate on failure path, defect, morphological and microstructural changes to propose way for improving TBC system lifetime.

## Introduction

Thermal barrier coatings are widely used in gas turbine engines. They are composed of a superalloy substrate with good mechanical properties, an Al rich bond coating (BC) which will form a protective alumina scale by reaction with oxygen and a top coat (TC) which should be strain tolerant and which is used to reduce the temperature seen by the entire system. If only thermal cycling conditions are considered, two failure categories can be distinguished for a TBC system [1]: intrinsic or extrinsic mechanisms. Intrinsic mechanisms are due to strain misfits between the different layers which compose a TBC system. They refer to rumpling and interface delamination. The other category is related to foreign particles. When these particles impact the top coat, this can be eroded or damaged (FOD). In the case where such particles would accumulate on the top coat surface and melt, top coat spallation will occur. In all cases, the top coat will be damaged and its beneficial effect on the TBC system will be lost. In the present study, the focus is on the intrinsic mechanisms which are rumpling and interface delamination. Thermal cycling tests of different TBC systems are then conducted, followed by Scanning Electron Microscopy (SEM) and Energy Dispersive Spectroscopy (EDS).

## Experimental Procedures

**Materials.** Two kinds of thermal barrier coating (TBC) systems were investigated. AM3 single crystal nickel-based superalloy was used as the substrate. The bond coating was either NiCoCrAlYTa or NiPtAl. The NiCoCrAlYTa bond coating was vacuum plasma sprayed (VPS).

After heat treatment, the microstructure is composed of  $\beta$ ,  $\gamma'$ ,  $\gamma$  and TaC phases. The NiPtAl BC was formed by platinum deposition via an electrolytic process followed by vapour phase aluminizing (APVS). After heat treatment, the bond coating is single-phase  $\beta$ -NiPtAl. The top coat, composed of  $\text{ZrO}_2$ -7wt% $\text{Y}_2\text{O}_3$ , was deposited by electron beam physical vapour deposition (EB-PVD) on grit blasted (NiPtAl) or partially machined (NiCoCrAlYTa) bond coatings. Bond coatings were preoxidized 3 h at 1000°C in air under 0.5 mbar before EB-PVD. Because of process requirement, a Hastelloy X stem was welded to the AM3 disc. The entire surface of the stem was also covered by the bond coating and the top coat except its extremity which was only covered by a NiCoCrAlYTa bond coating. More details about these systems can be found in [2, 3].

**Thermal cycling.** Before thermal cycling, specimens were oxidized 20 h at 1100°C or 900°C under flowing dry  $\text{O}_2$  in a thermobalance in order to measure the initial oxidation rates with precision. Then cyclic oxidation was performed using two devices: a SETARAM TAG24S thermobalance and a CTGA thermobalance. Due to its symmetrical furnace arrangement, the SETARAM TAG24S offers an excellent accuracy (about 1  $\mu\text{g}$ ) with limited drift and buoyancy effects. In one compartment, an inert alumina reference sample is placed, in the other one the TBC system under investigation. Then, the apparatus records the mass difference between the two specimens during thermal cycling, as detailed in [4]. The second apparatus was a CTGA thermobalance which was developed and patented in the laboratory [5]. Ten halogen lamps heat 5 independent samples whose weight is measured continuously. As a consequence, the initial heating and cooling of CTGA thermobalance are faster than those of the SETARAM TAG24S thermobalance. Nevertheless, both thermal cycles consisted of a high temperature dwell of 1 h at 1100°C and a 15 min cold dwell at 200°C (more details on thermal cycles are given in [3]). Thermal cycling was realized under flowing synthetic air (0.2-1 l/h for each sample). Both kinds of TBC systems were tested in both thermobalances. TBC29 and TBC30 samples have a NiPtAl bond coating, TBC47 and TBC48 samples a NiCoCrAlYTa bond coating. Specimens cycled in the SETARAM TAG24S thermobalance, TBC29 and TBC47, were oxidized for 20 h at 900°C before cycling. Samples cycled in the CTGA thermobalance, TBC30 and TBC48, were oxidized for 20 h at 1100°C before cycling. Thermal cycling is stopped at a certain number of cycles, depending on the system, before complete spallation determined by critical mass change.

## Results and Discussion

**Cyclic Oxidation Kinetics.** The thermobalances record net mass change. Oxidation kinetics and mass losses due to spallation can then be determined. Oxidation kinetics values were found to be characteristic of  $\alpha$ -alumina formation [3]. Fig. 1 shows the net mass change of each TBC system during thermal cycling. For easier interpretation of the results, only the net mass change at the end of each high temperature dwell is plotted. TBC48 spallation was severe and occurred very rapidly. For the other TBC systems, although oxidation kinetics are similar, spallation is more pronounced for TBC systems with a NiCoCrAlYTa bond coating.

**Systems degradation.** Samples were examined by SEM after thermal cycling (Fig.2). White areas represent the bond coating while black domains correspond to TGO. Bright regions on the top of TGO layer are top coat fragments. Whatever the bond coating and whatever the cycling duration, the bond coating, TGO and top coat are visible, as can be seen in Fig.2a and b. The bond coating shows alumina grain imprints which are characteristic of an inward growing oxide. The main difference is that the bond coating surface, which is highly convoluted in the case of a NiPtAl bond coating does not appear rumpled for a NiCoCrAlYTa bond coating, Fig.2c and d.

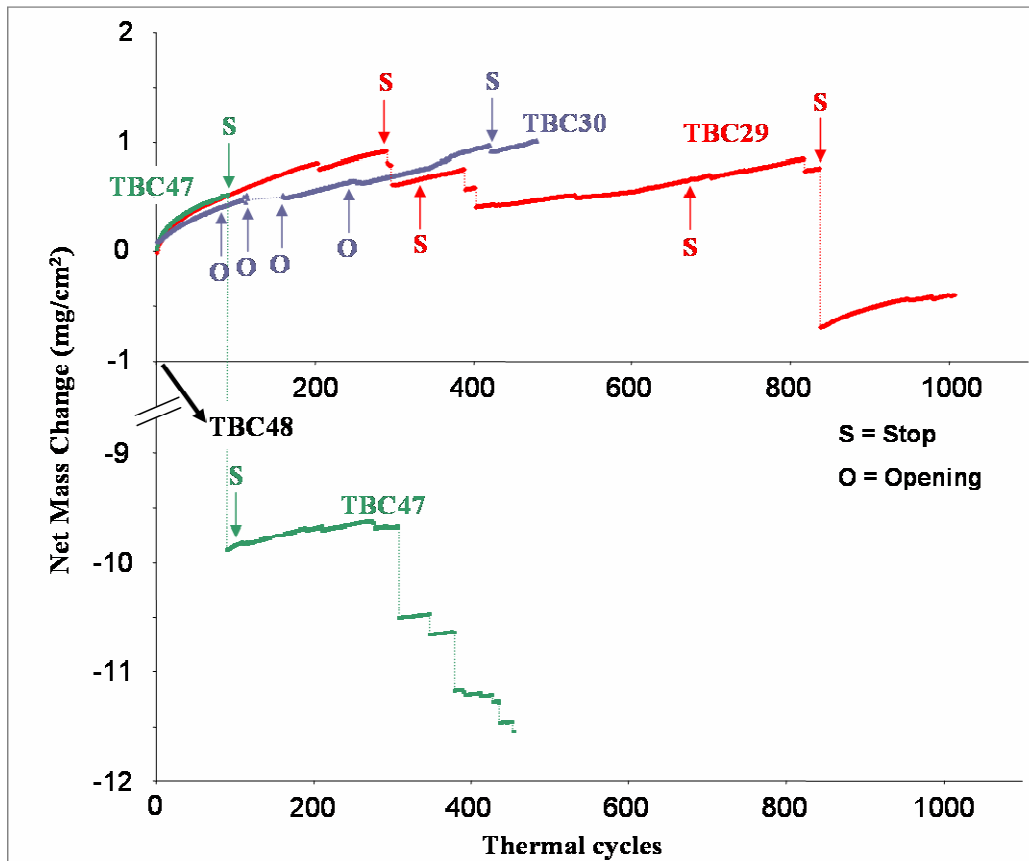


Fig. 1. Net Mass Change versus number of cycles. TBC29 and TBC30: NiPtAl BC, TBC47 and TBC48: NiCoCrAlYTa BC. S means that the thermal cycling was stopped. O means that the thermal cycling was stopped and that the furnace was open.

For both BCs, a major part of TGO layer has been lost during spallation. Nevertheless, dispersed remnant pieces of TGO are observed at the bond coating surface, Fig.2. In the case of a Pt-modified  $\beta$ -NiAl bond coating, the bond coating surface is severely rumpled. Then, by propagating along the BC/TGO interface, cracks can go through alumina layer in concave areas, Fig.3a. Such TGO remnants refer to ruptured ligaments [6]. In the case of a NiCoCrAlYTa bond coating, Y-rich oxides, Y, Ta-rich oxides and Ta,Ti-rich oxides are identified within TGO. Formation of reactive element compounds at the BC/TGO interface through which oxygen diffuses faster leads to enhanced oxidation, Fig.3b. Therefore, TGO is thicker in these regions which are usually called pegs, assuming that they mechanically peg the interface [7].

After spallation, zirconia appears showing two different shapes according to the bond coating. For NiPtAl, only remnants of zirconia base columns are still adherent to the top of ruptured ligaments, Fig.3c. For a NiCoCrAlYTa BC, zirconia is usually present as “corn kernel defect” [8] on the top of TGO, Fig.2d and 3d.

Cross section observations also highlight BC phase transformation, Fig.4. NiCoCrAlYTa bond coating is composed initially of  $\beta$ ,  $\gamma'$ ,  $\gamma$  phases with some TaC precipitates. After 80 cycles, it is still composed of  $\beta$ ,  $\gamma'$  and  $\gamma$  but it presents an external layer of  $\gamma$ , Fig.4a. After 456 cycles, the entire  $\beta$  phase disappeared and only  $\gamma$  and  $\gamma'$  are detected, Fig.4b. For Pt-modified  $\beta$ -NiAl, the coating was initially single-phased  $\beta$ . After 480 and 1007 cycles,  $\beta$ ,  $\gamma'$  and  $\gamma$  are present, Fig.4c and d. In both cases,  $\gamma$  is localized near BC/AM3 interface, a  $\gamma'$  layer develops under the TGO but  $\beta$  fraction decreases with oxidation time.

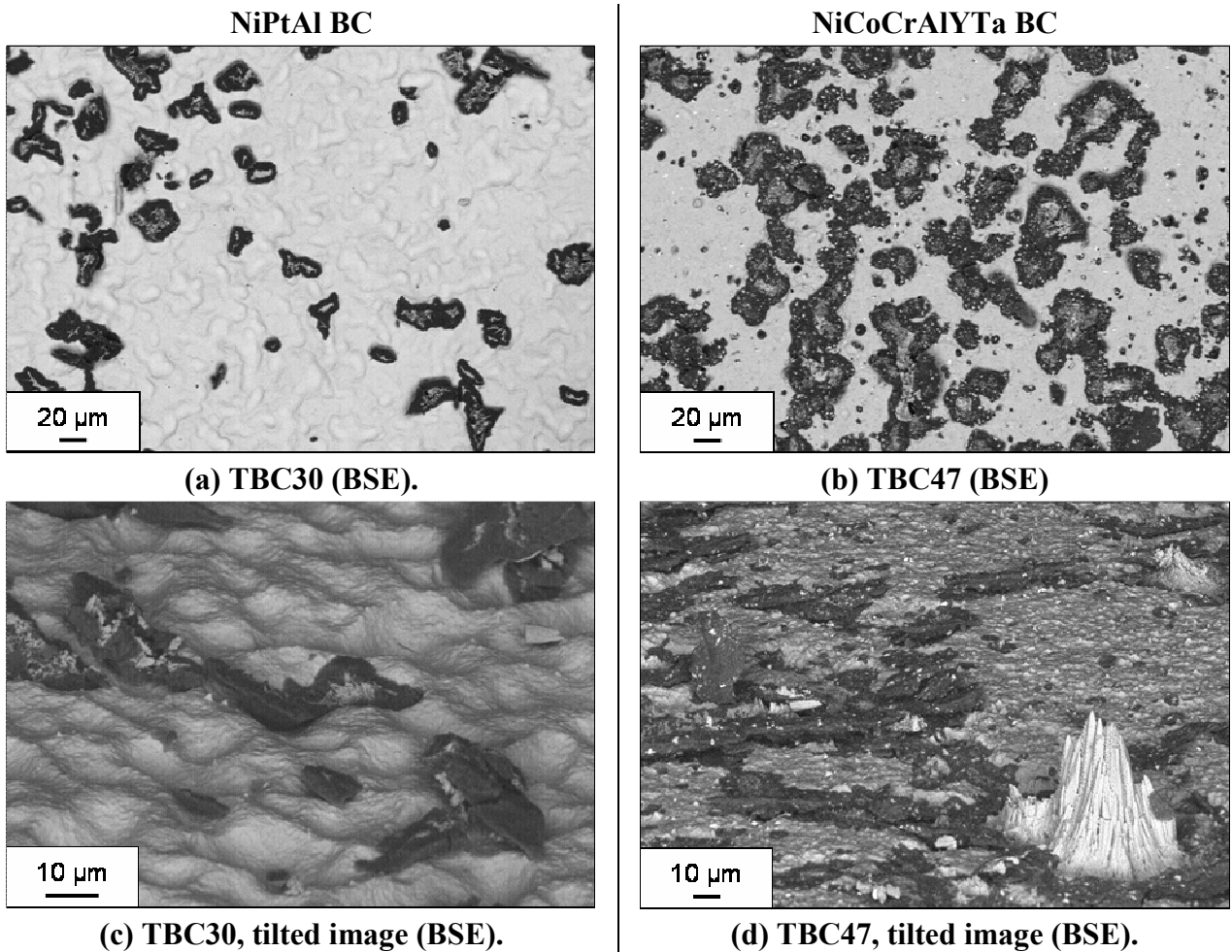


Fig. 2. Bond coating surface after thermal cycling (480 cycles for TBC30, 456 cycles for TBC47). Few parts of TGO and top coat remain on BC surface after spallation. Bond coating rumpling for TBC systems with Pt-modified  $\beta$ -NiAl BC (c), no rumpling for NiCoCrAlYTa BC (d).

It has been seen that whatever the bond coating of TBC systems is, failure mainly occurred at TGO/BC interface. Nevertheless, many differences were noticed between the two BC: rumpling vs. unconvoluted surface, pegs vs. anchorage points, corn kernel defects vs. base of zirconia columns, localised vs. homogeneous  $\beta$  transformation. All of these characteristics indicate that failure results from different mechanisms depending on the bond coating.

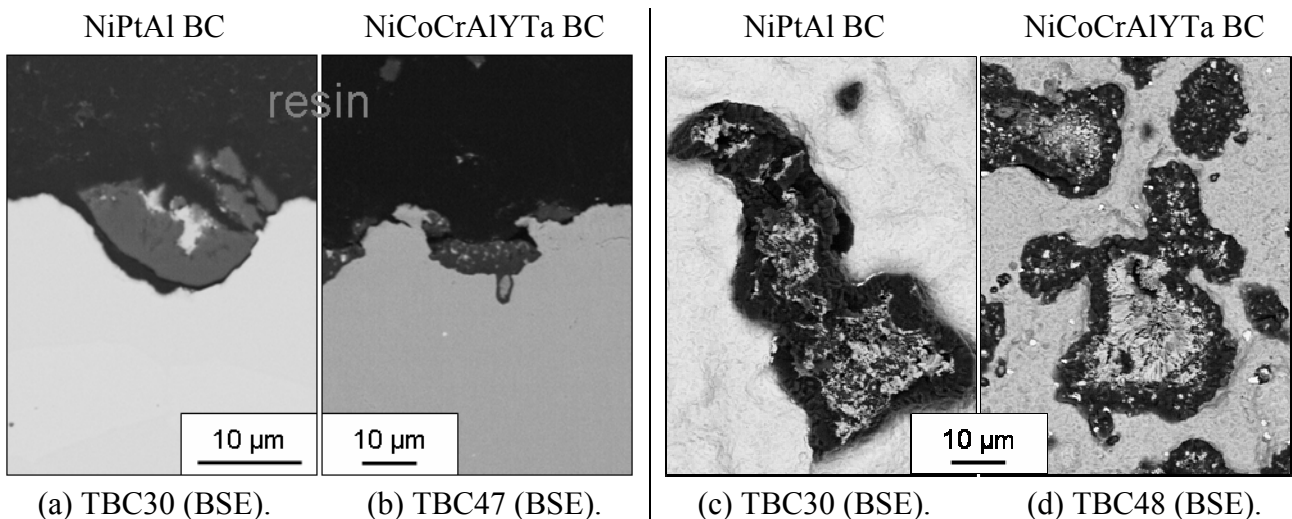


Fig. 3. a) Ruptured ligament, b) Peg. c) Base of  $ZrO_2$  columns and d) "corn kernel defect" on TGO.

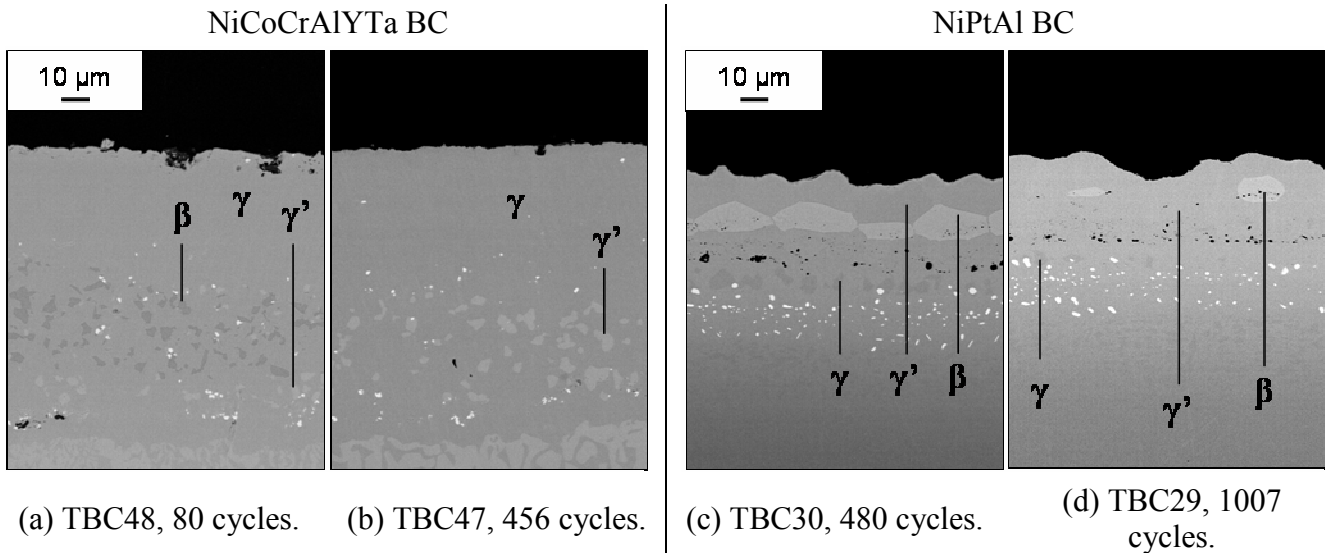


Fig. 4. Phases composition of bond coatings after thermal cycling, (BSE).

Surface undulations have been observed for MCrAlY BC without top coat only in a few studies [9, 10], but rumpling has often been observed in the case of NiPtAl BC with and without top coat, *e.g.* [11-13]. Different explanations have been given to explain such phenomenon. Compressive stress development within TGO is one of those and is mainly due to CTE mismatch. Besides, Pennefather and Boone [9] suggest that the mechanical strength of the coating could also play a role in rumpling whereas Evans *et al.* [14] assume that stresses due to TGO growth add to CTE mismatch in order to favor rumpling. Haynes *et al.* suggest that the CTE mismatch between the substrate and the BC has also to be taken into account [15]. But rumpling can also be related to phase transformation. Chen *et al.* [16] assume that the martensitic phase transformation is responsible for nickel aluminide coating rumpling. Tolpygo and Clarke claim that the  $\beta \rightarrow \gamma'$  transformation, which is associated with a volume change, can also explain the rumpling mechanism [13]. Vialas *et al.* [17] showed that this volume change can be either an increase or a decrease, and that the  $\beta/\gamma'$  phase transformation boundary can be either parallel to the surface or localized at BC grain boundaries. In the case of the present study, the attention is focused on this last explanation. The  $\beta \rightarrow \gamma'$  transformation can occur in such a way that a  $\gamma'$  layer forms continuously along the interface. Its penetration front gradually moves inward as the transformation continues and BC thickness remains uniform on the entire surface. If only a certain portion of  $\beta$  transforms locally to  $\gamma'$  and this is associated to a volume reduction, the BC surface can rumple or voids can form [13]. In the case of the NiCoCrAlYTa BC, Al consumption leads to the  $\beta \rightarrow \gamma$  instead of the  $\beta \rightarrow \gamma'$  transformation [18]. Given that such transformation occurs homogeneously, a continuous  $\gamma$  phase develops under the TGO/BC interface, Fig.4a and b. Besides, the  $\gamma/(\beta+\gamma'+\gamma)$  plane remains parallel to the interface as the transformation goes on. The formation of a continuous  $\gamma$  layer with a plane  $\gamma/(\beta+\gamma)$  was also observed in the case of a MCrAlY BC, initially biphased  $\beta+\gamma$  [19]. Then rumpling does not occur and TGO/TBC interface remains planar, Fig.5a. The only TGO layer deformation observed is related to the presence of corn kernel defects. These are conical defects within YSZ which are no longer bonded to the top coat. Consequently, bond coating deformation is not prevented at these specific locations [12] and TGO imperfections due to undulations develop [14]. Such BC deformation due to corn kernel defects has already been observed by Sohn *et al.* [19] in the case of MCrAlY bond coating TBC systems. Concerning NiPtAl BC, the rumpling of the surface is the result of the volume reduction associated with the localized transformation, Fig.4c and d. When TGO is adherent on the BC, it follows the

bond coating surface undulations and imperfections due to a convoluted TGO are then created [14]. Out of plane stresses develop and cracks nucleate around concave and convex areas, Fig.5b. The large fraction of BC surface observed suggests that these cracks go through the TGO in order to reach and propagate at the TGO/BC interface where the release of stored energy is more important [8]. Rumpling is then responsible for the failure of TBC systems with a NiPtAl BC even though this allows a decrease in the TGO elastic strain, as assumed by Tolpygo *et al.* [12]. Such failure path (cracks initiated at TGO/TC interface which propagate at TGO/BC interface) has already been observed by Tolpygo and Clarke on a TBC system composed of a René N5 superalloy and a Pt-modified nickel aluminide BC after thermal cycling [13].

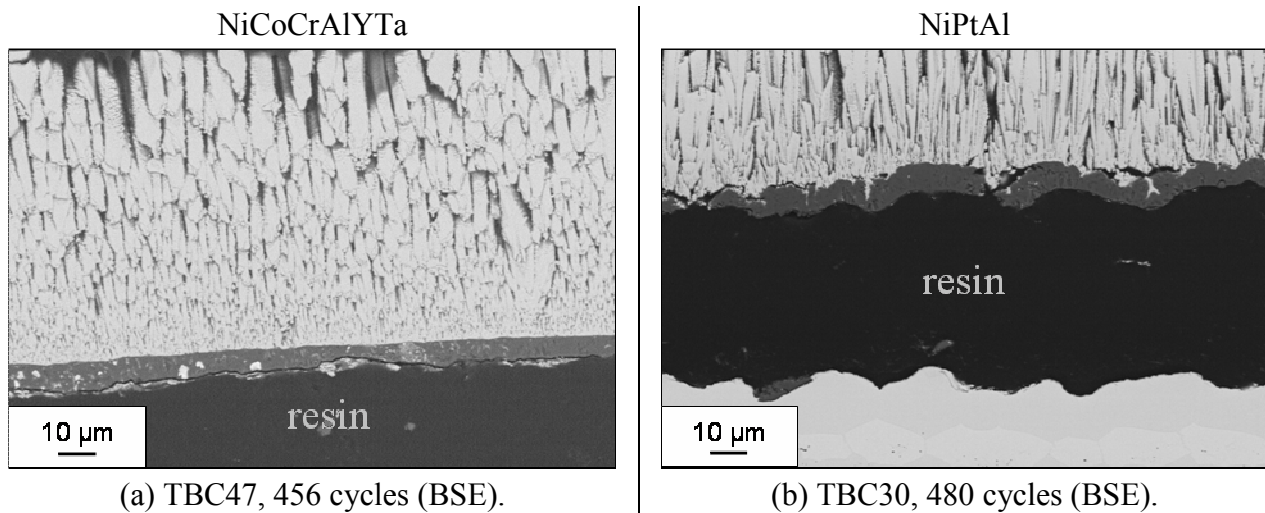


Fig. 5: Interface between TGO/top coat for both bond coatings.

It is worth mentioning that such a failure mechanism occurs for the entire surface of TBC30 but for only 70% of the TBC29 surface (after 1007 thermal cycles). Actually, on the other 30% of the surface of TBC29, the TGO layer was still adherent to the BC and appeared much more convoluted than the BC surface without TGO. Fig. 6a is a top view of the TGO layer where it is still adherent to the BC. This strong rumpling increases TGO length and consequently Al consumption. Therefore, it is not surprising to discover  $\gamma$  phase just below the TGO/BC interface in convex areas, Fig.6b. On the top of this TGO layer, the base of zirconia columns is observed but only at few places. This suggests that cracks coalesce at the TGO/TC interface but cannot propagate along the complete interface because top coat is still adherent to the TGO where the base of zirconia columns is observed. Given that top coat cannot constrain TGO undulations anymore, the TGO is free to rumple. This explains why rumpling is much more important here than in the areas where TGO is no longer adherent to the bond coating. Finally, if no large mass loss is detected during TGA measurement, it is because TGO/TC interface is still adherent at few points, preventing it from spalling.

Rumpling for TBC systems with a NiPtAl BC, and corn kernel defects for TBC systems with a NiCoCrAlYTa BC, are both responsible, in different ways, for TGO undulations. In the case of a NiCoCrAlYTa BC, another important feature with regard to the TGO microstructure and morphology is the important formation of pegs. As mentioned previously, pegs develop because of the presence of yttrium oxides which locally increase oxidation kinetics [20, 21]. Like other reactive elements (Hf, Zr) [21, 22], yttrium is known to have a beneficial effect on the TGO adherence. This effect is attributed to many different mechanisms, the most important of which is the impurity gettering [22]. But the beneficial effect of reactive elements is highly linked to their concentration.

A study of Haynes *et al.* [15] on cyclic oxidation of various MCrAl BC clearly reveals that lifetime and TGO adherence are strongly dependent on reactive element concentration within the coating, as shown also by Lau *et al.* [23]. According to Toscano *et al.*, the Y reservoir has to be sufficient in order to favor TGO adherence but it must not be too high in order to avoid large oxidation kinetics [20]. Two alternative explanations have been offered for the pegs effect. Nijdam *et al.* [24, 25] consider that the pegs density has to be important to prevent crack propagation whereas in a study on the effect of Y or Hf implantation in nickel aluminide coatings, Fisher *et al.* conclude that spallation was due to excessive Hf-rich peg formation [26]. Besides, pegs create TGO thickness imperfections [14]. As mentioned by Yanar *et al.*, defects in TBC systems are initiation sites and the stored energy in the TGO is the driving force for the failure propagation [8]. Consequently, a large and non-uniform TGO thickness is not favorable given that the strain energy will be more important and the failure probability increased. If we refer to the statement of Yanar *et al.*, defects and TGO thickness have to be limited to improve TBC system lifetime. In the present study, TBC systems with NiCoCrAlYTa BC present many defects: corn kernel defects which cause a localized BC deformation and many TGO imperfections. All these defects, associated with a high strain energy due to pegs, are responsible for the short TBC system lifetimes.

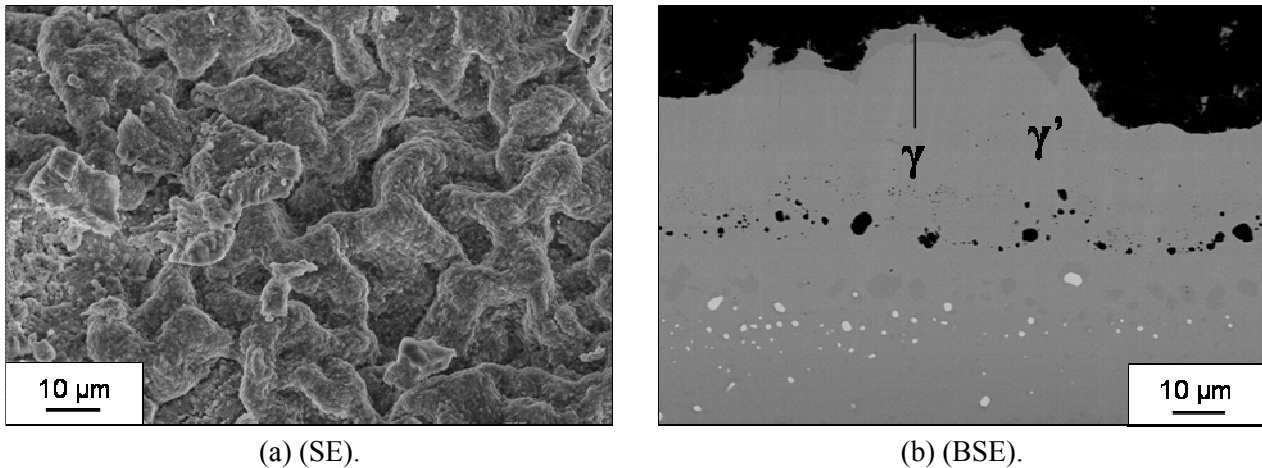


Fig. 6: TBC29 after 1007 cycles (NiPtAl bond coating). (a) TGO remains adherent to the bond coating in some areas and is highly convoluted. (b) This leads to the  $\gamma' \rightarrow \gamma$  transformation.

Corn kernel defects result from initial BC surface roughness [8]. In the present case, rumpling is likely to be due to BC composition and microstructure. The formation of pegs is caused by BC surface roughness and composition. The fact that peg formation is caused by BC composition has already been explained previously. But other works have shown that the surface preparation also plays an important role on the lifetime of TBC systems. Indeed, two studies on MCrAlY, one by Naumenko *et al.* [27] and the other one by Gil *et al.* [28], show the importance of surface preparation on TGO morphology and composition. A rough surface will favor peg formation and development of a non-uniform TGO while a uniform TGO, in composition and microstructure, forms on an almost planar surface. Then, two ways to improve TBC systems durability can be undertaken. The first one is based on an accurate control of BC composition and microstructure. In the case of a nickel aluminide BC, efforts are to be made to avoid rumpling. Using a  $\gamma+\gamma'$  bond coating [29] can offer the advantages of having a CTE and a composition closer to those of the superalloy. Besides, the two-phased composition of the bond coating might minimize rumpling. In the case of MCrAlY BC, reactive elements have to be added for their beneficial effect on scale adherence without leading to excessive peg formation. The second way to improve the TBC



systems lifetime is to minimize defects by controlling the surface roughness and consequently by using the appropriate surface preparation, as already shown by Yanar *et al.* [8]. However, BC surface must not be too smooth otherwise nothing can prevent fast crack propagation. Thus, the formation of a limited number of pegs could be a good compromise with regards to crack propagation given that pegs roughen the interface.

## Conclusion

The composition of the bond coating plays a major role in determining the failure mechanism of a TBC system. In the case of a TBC system with a Pt-modified bond coating, failure is mainly caused by rumpling. For a TBC system with a NiCoCrAlYTa bond coating, the high density of defects and TGO heterogeneities are found to be responsible for top coat spallation with shorter lifetimes than the NiPtAl-base system. Such defects result from bond coating surface roughness before EB-PVD. TGO heterogeneities come from reactive element rich oxide formation. Consequently, bond coating surface preparation and also the reactive element reservoir within the bond coating have to be carefully controlled in order to increase TBC system lifetime.

## Acknowledgments

Turboméca-SAFRAN (F. Crabos and A. Raffaitin) and Snecma Services-SAFRAN (A. Malié) companies are gratefully acknowledged for providing TBC samples, Turboméca and CNRS for financial support of A. Vande Put PhD.

## References

- [1] B. Gleeson: J. of Propulsion and Power Vol. 22 (2006), p. 375
- [2] D. Monceau, F. Crabos, A. Malie, B. Pieraggi: Mater. Sc. Forum Vol. 369-372 (2001), p. 607
- [3] A. Vande-Put, D. Monceau, D. Oquab: Surf & Coat. Technol. (2007) , in press
- [4] D. Monceau, D. Poquillon: Oxid. Met. Vol. 61 (2004), p. 143
- [5] J.C. Salabura, D. Monceau, Mater. Sc. Forum Vol. 461-464 (2004), p. 689-696
- [6] D.R. Mumm, A.G. Evans: Acta Mater. Vol. 48 (2000), p. 1815
- [7] D.P. Whittle, J. Stringer: Phil. Trans. R. Soc. London Vol. A295 (1980), p. 309
- [8] N.M. Yanar, F.S. Pettit, G.H. Meier: Met. Mater. Trans. A Vol. 37A (2007), p. 1563
- [9] R.C. Pennefather, D.H. Boone: Surf. & Coat. Technol. Vol. 76-77 (1995), p. 47
- [10] L. Peichl, D.F. Bettridge, Proc. Materials for Advanced Power Engineering Conf., Part I, Eds. D. Coutsouradis *et al.*, Kluwer (1994), p. 717
- [11] V.K. Tolpygo, D.R. Clarke: Surf. & Coat. Technol. Vol. 163-164 (2003), p. 81
- [12] V.K. Tolpygo, D.R. Clarke, K.S. Murphy: Surf. & Coat. Technol. Vol. 188-189 (2004), p. 62
- [13] V.K. Tolpygo, D.R. Clarke: Acta Mater. Vol. 48 (2000), p. 3283
- [14] A.G. Evans, D.R. Mumm, J.W. Hutchinson, G.H. Meier, F.S. Pettit: Prog. Mater. Sci. Vol.46 (2001), p. 505

- [15] J.A. Haynes, B.A. Pint, W.D. Porter, I.G. Wright: *Mater. High Temp.* Vol. 21 (2004), p. 87
- [16] M. Chen, M.L. Glynn, R.T. Ott, T.C. Hufnagel, K.J. Hemler: *Acta Mater.* Vol. 51 (2003), p. 4279
- [17] N. Vialas, D. Monceau: *Oxid. Met.* (2007), in press
- [18] A. Taylor, R.W. Floyd: *J. Inst. Metal.* Vol. 81 (1952), p. 451
- [19] Y.H. Sohn, J.H. Kim, E.H. Jordan, M. Gell: *Surf. & Coat. Technol.* Vol. 146-147 (2001), p. 70
- [20] J. Toscano, R. Vaßen, A. Gil, M. Subanovic, D. Naumenko, L. Singheiser, W. J. Quadakkers: *Surf. & Coat. Technol.* Vol. 201 (2006), p. 3906
- [21] J. Toscano, D. Naumenko, A. Gil, L. Singheiser, W. J. Quadakkers: *Materials and Corrosion* (2007), in press
- [22] B.G. Mendis, K.J.T. Livi, K.J. Hemker: *Scripta Mater.* Vol. 55 (2006), p. 589
- [23] H. Lau, C. Leyens, U. Schulz, C. Friedrich: *Surf. & Coat. Technol.* Vol. 165 (2003), p. 217
- [24] T.J. Nijdam, W.G. Sloof: *Surf. & Coat. Technol.* Vol. 201 (2006), p. 3894
- [25] T.J. Nijdam, G.H. Marijnissen, E. Vergeldt, A.B. Kloosterman, W. G. Sloof: *Oxid. Met.* Vol. 66 (2006), p. 269
- [26] G. Fisher, P.K. Datta, J.S. Burnell-Gray, W.Y. Chan, J.C. Soares: *Surf. & Coat. Technol.* Vol. 110 (1998), p. 24
- [27] D. Naumenko, M. Subanovic, M. Kamruddi, E. Wessel, L. Niewolak, L. Singheiser, W.J. Quadakkers: submitted
- [28] A. Gil, V. Shemet, R. Vassen, M. Subanovic, J. Toscano, D. Naumenko, L. Singheiser, W. J. Quadakkers: *Surf. & Coat. Technol.* Vol.201 (2006), p. 3824
- [29] V. Deodshmikh, N. Mu, B. Li, B. Gleeson: *Surf. & Coat. Technol.* Vol.201 (2006), p. 3836